Article

Lipidomic Analysis on Gender-Dependent Hepatocellular Carcinogenesis in Hras12V Transgenic Mice

Juefu Hu , Huiling Li , Nan Mao , Huaiyuan Di , Yanan Zhao , Jun Chen [*] , Aiguo Wang [*]

Article

Lipidomic Analysis on Gender-Dependent Hepatocellular Carcinogenesis in Hras12V Transgenic Mice

Juefu Hu [1,2,†], **Huiling Li** [1,†], **Nan Mao** [1], **Huaiyuan Di** [1], **Yanan Zhao** [1], **Jun Chen** [1,*] **and Aiguo Wang** [1,*]

1   Department of Comparative Medicine, Laboratory Animal Center, Dalian Medical University, Dalian, Liaoning 116044, China; hujuefu@outlook.com (J.H.); lhl@dmu.edu.cn (H.L.); maomunan@outlook.com (N.M.); huaiyuandi2116@outlook.com (H.D.); yananzhao4869@outlook.com (Y.Z.)

2   School of Pharmacy, Hubei University of Chinese Medicine, Wuhan 430065, China

*   Correspondence: chenjun@dmu.edu.cn (J.C.); wangaiguo@dmu.edu.cn (A.W.); Tel.: +86-411-86110171; Fax: +86-411-86110172

†   The two authors contributed equally to this work.

Abstract: Lipid dysregulation is critically involved in hepatocellular carcinoma (HCC). Further, male predilection and Ras pathway hyperactivation are distinct characteristics of HCC. However, mechanisms underlying their connections remain unknown. The aim of the present study was to perform a comprehensive lipidomics analysis of a Hras12V transgenic mice (Ras-Tg) model of HCC induced by hepatocyte-specific Ras pathway activation and characterized by male predilection and a disrupted lipid metabolism. A total of 3437 lipids were identified in HCC (T) and peri-tumor tissues (P) of Ras-Tg mice and liver tissues of wild-type mice (W) of both sexes. Longitudinal comparisons of W, P, and T yielded 359 differentially expressed lipids (DELs) in male mice and 306 DELs in female mice. Generally, glycerolipid accumulation, glycerophospholipid reduction and monounsaturated fatty acid synthesis improvement were more frequent in T compared to P. The expression change pattern analysis revealed common and characteristic DELs positively/negatively associated with HCC or the *Ras* oncogene. Further lipid metabolism pathway investigations revealed that disordered lipid and fatty acid biosynthesis contributed to glycerolipid accumulation and glycerophospholipid reduction in T. Comparisons between P and W suggests that different responses to the *Ras* oncogene in mice of different sexes, as well as higher amounts of aberrantly regulated lipids in males, may contribute to male-biased hepatocarcinogenesis. However, lateral comparisons between sexes showed a converging trend during hepatocarcinogenesis, explaining the poor efficacy for gender-specific therapies. In conclusion, the common and characteristic DELs and lipid metabolism pathways in HCC initiated by the *Ras* oncogene from sexually dimorphic hepatocytes provide novel insights into the clinical diagnosis and management of HCC.

Keywords: lipidomics; hepatocellular carcinoma; *Ras* oncogene; sex disparity

1. Introduction

Hepatocellular carcinoma (HCC), accounting for over 90% cases of primary liver tumors, is a common malignant tumor. Its occurrence is a complex process with multiple etiologies and steps. Risk factors include viral hepatitis (hepatitis B and C), alcoholic liver disease, male sex, and non-alcoholic fatty liver disease (NAFLD) [1]. HCC with NAFLD without advanced fibrosis is more common in men than in women and characterized by large tumor size [2]. However, few studies have identified lipid reprogramming features of HCC genesis with gender disparity.

Energy metabolism changes are the cornerstone of hepatocellular tumor initiation and adaptation [3]. In addition to activating glycolysis, lipid metabolism reprogramming helps hepatoma deal with metabolic stress, as evidenced by increased fatty acid (FA) oxidation, and highly depends

on lipids through external uptake and *de novo* lipogenesis [4]. Additionally, the multiple functions of lipids in cell signaling and membrane composition are also critical to cancer cells [5]. Lipids can promote tumor activity [6]. Therefore, studies on the role of lipid metabolism in HCC could explain tumor occurrence and development. Lipidomicsis a main branch of metabolomics proposed in 2003 [7]. In recent years, non-targeted lipidomic approaches have been widely used in the study of various liver diseases to search for disease and drug mechanisms or key lipid biomarkers. However, the research of lipid metabolism disorders in sex-biased HCC is limited.

Ras signal transduction pathway abnormalities are associated with many cellular processes, such as cell survival and proliferation, and commonly involved in malignant transformation, including to HCC [8]. The Ras pathway is ubiquitously activated in HCC [9] and plays a prognostic role. *Raf-1* and *pMEK1* are overexpressed in patients with HCC with short survival, and *Raf-1* overexpression is an independent biological marker for early tumor recurrence and poor prognosis [10]. The relationship between the Ras pathway and lipids is intertwined and multifaceted. For example, Ras modulates tumor invasion and metastasis by regulating the lipid metabolism; FAs help cope with Ras oncogenic stress; lipids reversibly regulate the localization and function of Ras proteins [11]. However, the revealed correlations require further investigation.

In the present study, lipidomics was performed on a Hras12V transgenic (Ras-Tg) mice model of HCC induced by liver-specific activation of the Ras signal pathway with characteristics of lipid metabolism disorder and male predilection [12,13]. The revealed systematic feature of lipid expression profiles in *Ras* oncogene-induced hepatocarcinogenesis with sex disparity casts new lights on our understanding of the underlying intracellular mechanisms in male-biased HCC.

2. Results

2.1. Workflow and validation of the quality of lipidomics data

Figure 1A shows the workflow of the present study. We selected 9-month-old male and 15-month-old female Ras-Tg mice because their HCCs had similar development stages and sizes (Figure 1A,B) [12,14]. There was no pathological damage to liver tissue of wild type mice (Figure 1B).

Ultra-performance liquid chromatography-tandem mass spectrometry (UPLC-MS/MS) identified a total of 3437 lipid metabolites in both positive and negative ion modes (Table S1). The precision of the overall analytical method was evaluated by the calculation of relative standard deviation (RSD) of the quality control (QC) samples and the observation of their distribution (Figure S1). Principal component analysis (PCA) score plots showed separation among different groups in males and females, respectively (Figure 1C). All samples scattered in PCA score plots were within the 95% confidence interval. Consistently, the unsupervised hierarchical clustering of lipidomics data demonstrated well clustering in the same group and separation among different groups (Figure 1D). These data indicated that the qualities of the obtained samples and corresponding UPLC-MS/MS data were satisfactory for further lipidomics.
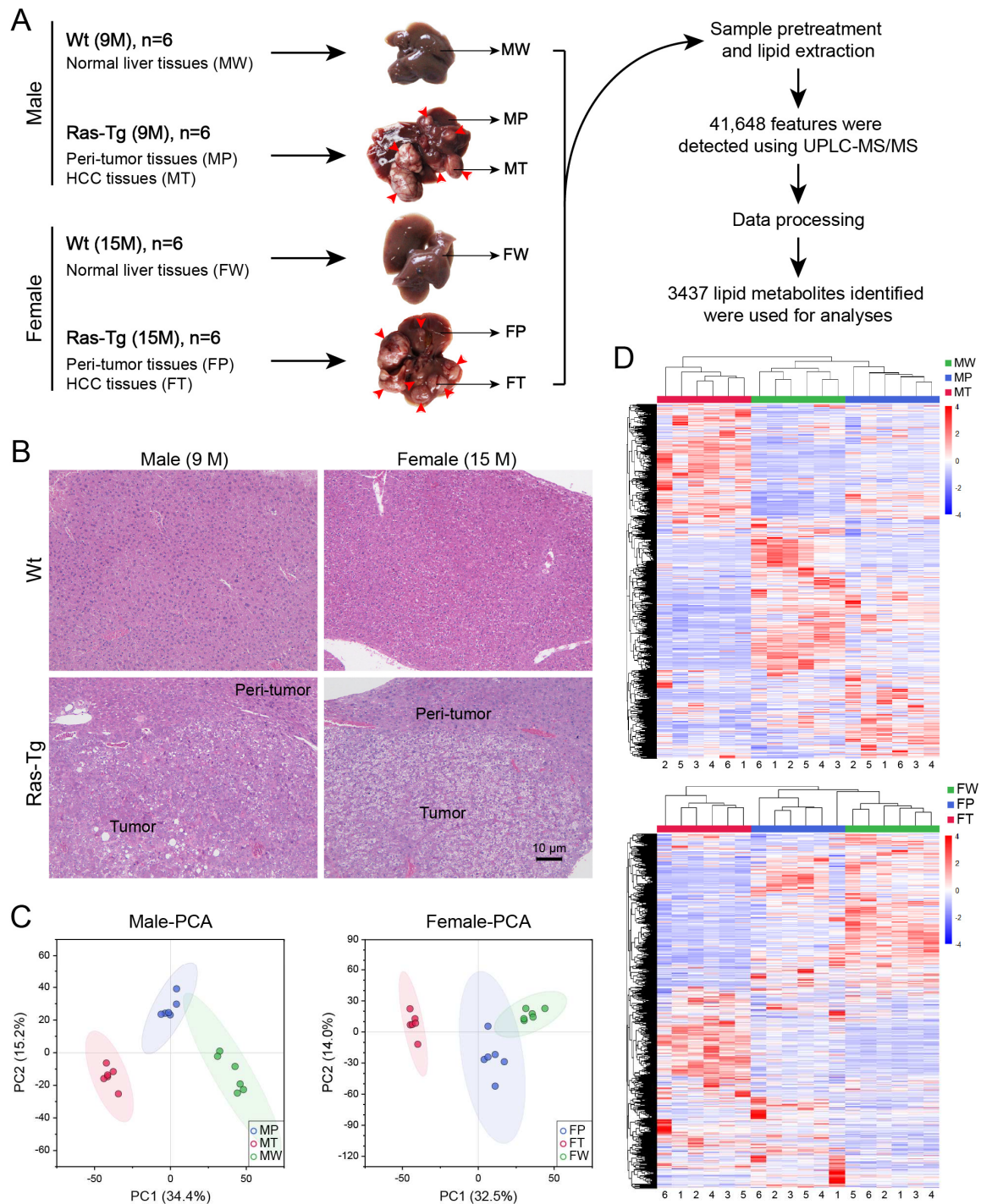
Figure 1. Workflow and validation of the quality of lipidomics data. (**A**) The workflow and representative liver stereogram images. The red arrows indicate hepatic alterations. (**B**) Representative hematoxylin and eosin-stained images (magnifications: 100×). (**C**) PCA score plots based on lipidomics data. Green circles, wild-type liver tissues; blue circles, peri-tumor tissues; red circles, HCC tissues. (**D**) Unsupervised hierarchical clustering based on lipidomics data. Red and blue show higher and lower lipid levels, respectively. F, female; M, male; Wt, wild-type mice; Ras-Tg, Hras12V transgenic mice; W, liver tissues of Wt; P, peri-tumor tissues of Ras-Tg; T, HCC tissues of Ras-Tg; 9M, 9-month-old; 15M, 15-month-old. n = 6.

2.2. Lipid composition analysis

The categories of lipid metabolites identified, as well as the subclasses, are shown in Figure S1F. To investigate changes in lipid levels in sex-dependent hepatocarcinogenesis induced by the *Ras*

oncogene, the proportions of lipid categories and their major subclasses were analyzed (Figure S2). Although W differed much in sexually dimorphic lipid composition, the differences narrow in peri-tumor tissue (P) and HCC (T) of Ras-Tg mice. It indicates that the *Ras* oncogene expression and HCC development significantly reprogrammed lipid metabolisms and diminished sex disparities. In addition, the distinct lipid compositions in W, P, and T indicated the requirement of lipid metabolisms for normal functioning of the liver, responses to the *Ras* oncogene, and HCC development, respectively.

Since glycerolipids, glycerophospholipids, and sphingolipids are the main lipid categories involved in hepatocarcinogenesis, changes in the level of their main subclasses were further analyzed (Figure 2).
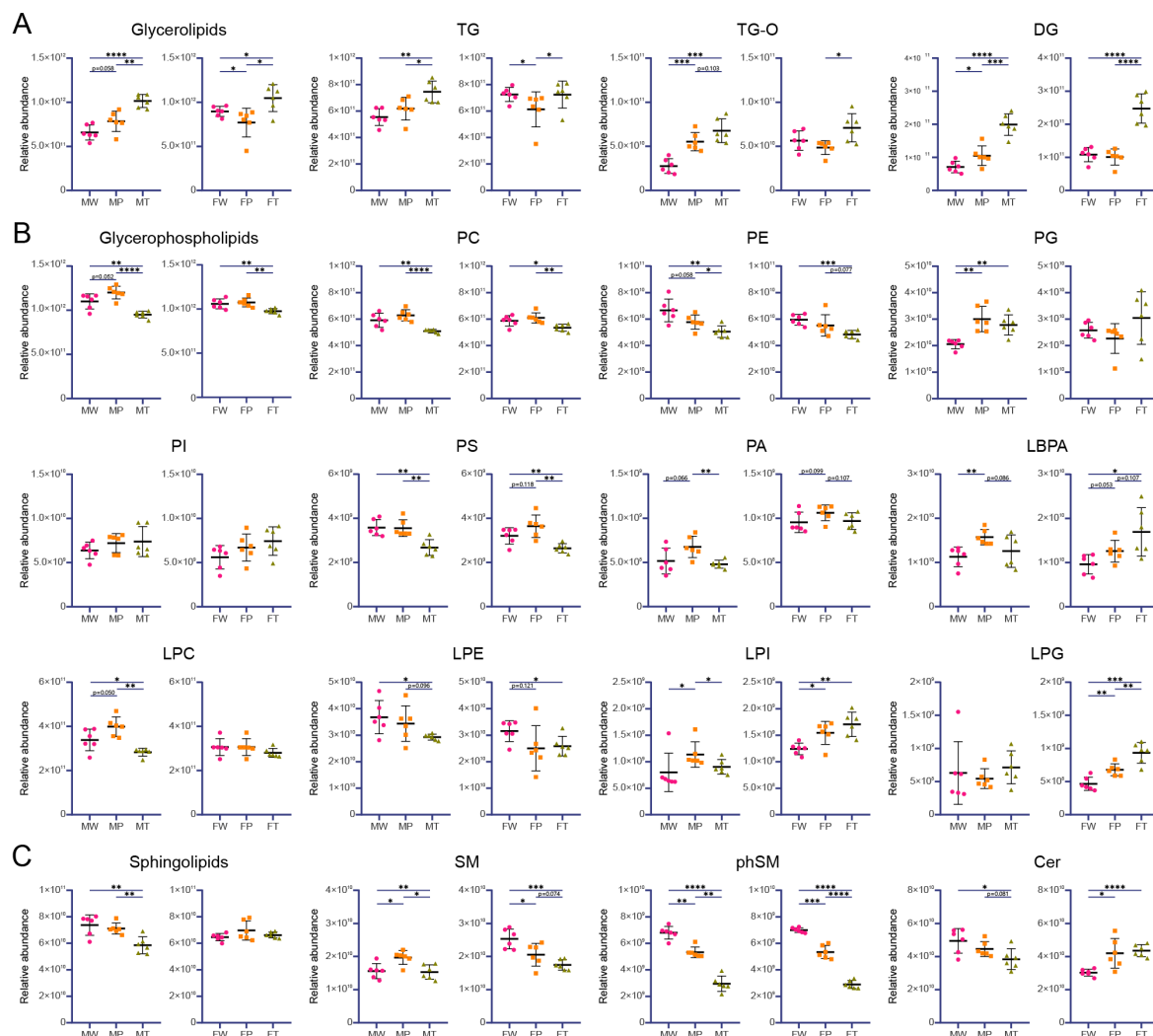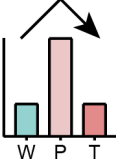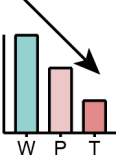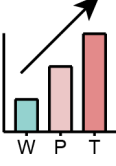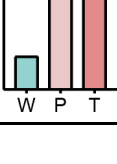

Figure 2. Major lipid level changes during hepatocarcinogenesis. (**A**) Glycerolipids and its major subclasses triacylglycerol (TG), alkyldiacylglycerol (TG-O) and diacylglycerol (DG). (**B**) Glycerophospholipids and its major subclasses phosphatidylcholine (PC), phosphatidylethanolamine (PE), phosphatidylglycerol (PG), phosphatidylinositol (PI), phosphatidylserine (PS), phosphatidic acid (PA), lysobisphosphatidic acid (LBPA), lysophosphatidylcholine (LPC), Lysophosphatidylethanolamine (LPE), Lysophosphatidylinositol (LPI) and lysophosphatidylglycerol (LPG). (**C**) Sphingolipids and its major subclasses sphingomyelin (SM), phytosphingosine (phSM), ceramide (Cer). The abbreviations as well as descriptions are the same as those in the caption for Figure 1. The data are expressed as the mean ± SD. *, $p < 0.05$; **, $p < 0.01$; ***, $p < 0.001$; ****, $p < 0.0001$. n = 6.

Although some changes did not reach statistical significance, lipid level changes during hepatocarcinogenesis could be summarized into eight basic models (Table 1). In addition, pairwise comparisons between males and females indicated that the sex disparity in lipid levels narrowed in P and T (Table S2). Generally, these findings indicated sexually dimorphic lipid composition in W, different responses to the *Ras* oncogene in P, and a converging trend in T between sexes.

Table 1. Lipid level changes during hepatocarcinogenesis.

Models	Description	Regulated Lipids	
		Male	**Female**
	First reduced in P and then elevated in T		Total glycerolipid, TG
	First elevated in P and then reduced in T	Total glycerophospholipid, PA, LBPA, LPC, LPI, SM	PS, PA
	Continuous reduced in P and T	PE, phSM	SM, phSM
	Continuous elevated in P and T	Total glycerolipid, TG-O, DG	LBPA, LPG
	Unchanged between W and P but reduced in T	Total sphingolipid, PC, PS, LPE, Cer	Total glycerophospholipid, PC, PE
	Unchanged between W and P but elevated in T	TG	TG-O, DG
	First reduced in P and then remained in T		LPE
	First elevated in P and then remained in T	PG	LPI, Cer

2.3. Accumulation of saturated FA (SFA) and monounsaturated FA (MUFA) in hepatic carcinogenesis

Rearrangement of fatty acids is an important feature of cancer, so the levels of SFA, MUFA, and polyunsaturated fatty acids (PUFA) bound to all lipids as well as those bound to the most abundant glycerolipid subclasses (DG, TG, and TG-O) and glyceroglycerophospholipid subclasses (PC, LPC, and PE) were analyzed (Figures 3A and S3A). Although changes in SFA and PUFA levels during hepatic carcinogenesis differed between sexes, SFA and MUFA levels in T of both males and females were elevated relative to P. In addition, complex and regular changes in the ratios of these fatty acids in all lipids, as well as in the most abundant lipid subclasses, such as a decrease in PUFA/SFA in all lipid species (with the exception of TG in males), suggest a role for altered lipid unsaturation in carcinogenesis (Figures 3B and S3B). Particularly, sexually dimorphic lipid unsaturation was a key factor causing sex disparity in change patterns.

Analysis of all lipid-bound FA chains showed that the species leading to significantly higher SFA and MUFA in T than in P were palmitic (16:0) and oleic acids (18:1) (Figure 3C). Therefore, changes in transcript levels of FA biosynthesis, desaturation, and exogenous uptake pathways were examined by RT-qPCR. The results showed that the desaturase *Scd2* was significantly elevated in T compared with P, resulting in increased oleic acid synthesis. In addition, *Lpl*, *Acsl4* and *Acsl5* may enhance the accumulation of these FAs in HCC through uptake and biosynthesis (Figures 3D). Data for W were not included in Figure 3D because of the complex situations in W between sexes relative to P and/or T.
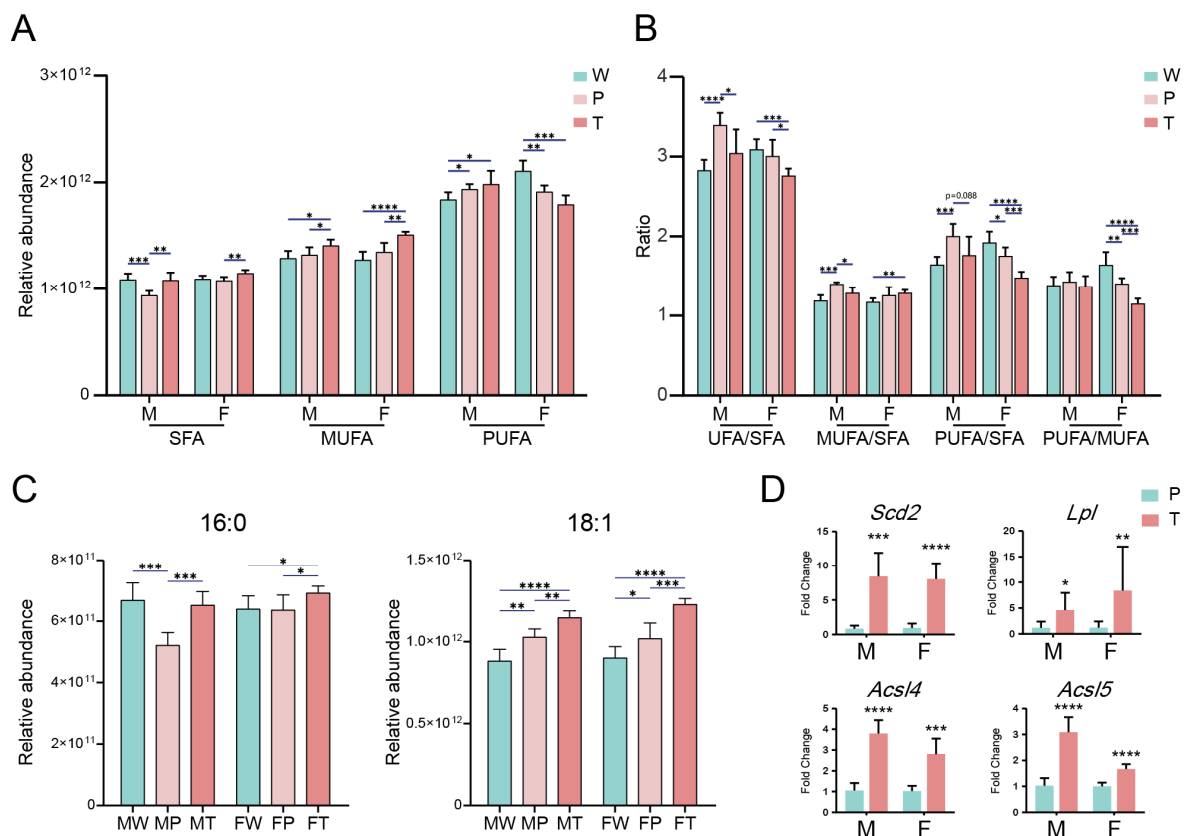
Figure 3. Accumulation of SFA and MUFA in hepatic carcinogenesis. (**A**) Levels of SFA, MUFA, and PUFA in W, P, and T of female and male mice. (**B**) UFA/SFA, MUFA/SFA, PUFA/SFA and PUFA/MUFA ratios in W, P, and T tissues of female and male mice. (**C**) Lipid-bound palmitic (16:0) and oleic (18:1) acids were significantly elevated in T relative to P in both sexes. (**D**) RT-qPCR results of the expression levels of the related key enzymes. The abbreviations as well as descriptions are the same as those in the caption for Figure 1. The data are expressed as the mean ± SD. *, $p < 0.05$; **, $p < 0.01$; ***, $p < 0.001$; ****, $p < 0.0001$. n = 6.

2.4. Identification of deferentially expressed lipids (DELs)

Combining multivariate statistical analyses, such as the orthogonal projections to latent structures discriminant analysis (OPLS-DA), with univariate statistical analyses is reliable for screening differential metabolites [15]. In this study, 514 lipids in male mice and 482 lipids in female mice (Table S3) were selected as DELs among the identified lipids by combining the univariate analysis (Figure S4) and OPLS-DA (Figure S5) based on the criteria of $p < 0.05$, fold change > 1.5, and variable importance of projection (VIP) > 1.

The number of DELs in paired comparisons among W, P, and T of male and female mice were first analyzed (Figure 4A). The number of total DELs was higher in male mice than in female mice, similar to our previous proteomics investigations [16]. Interestingly, the number of DELs in P/W was much higher in males (266) than in females (227), particularly upregulated DELs (140 vs. 83). To clarify changing trends in lipid levels during hepatocarcinogenesis, the main lipid subclasses DG, TG, TG-O, PC, LPC, PE, PG, Cer and SM were further analyzed based on DELs (Figure 4B). Consistently, the change trends of most of these DEL subclasses were similar to their overall change trends (Figure 2). Generally, between the sexes, glycerolipids, glycerophospholipids and sphingolipids showed similar trends in T/P, whereas their changes in P/W were complex. These data indicated that lipid metabolism is sex-dependent, and males are more susceptible than females to interference with *Ras* oncogene during hepatic carcinogenesis, reflecting the mechanism of male preference for HCC.
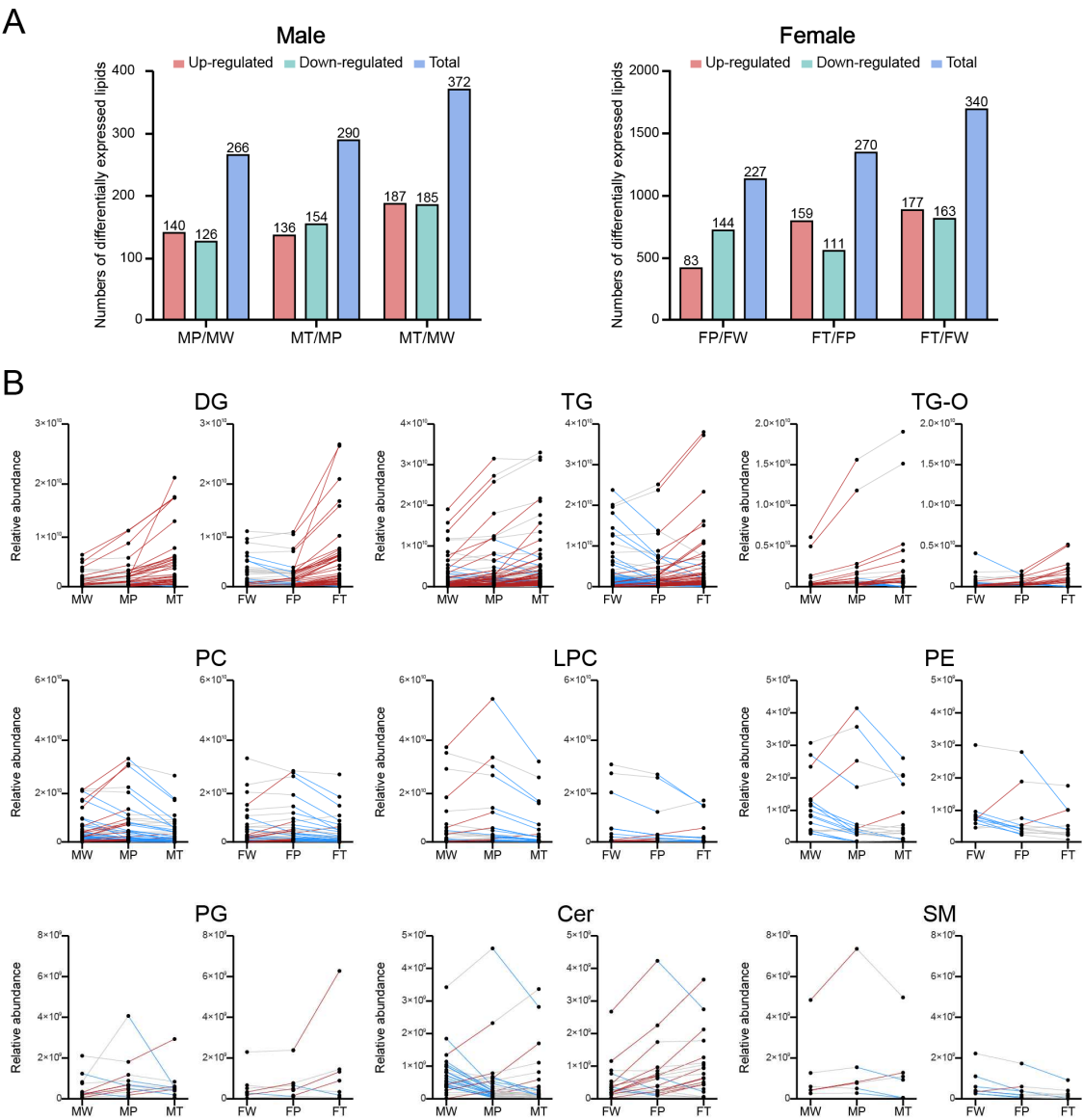
Figure 4. Number and change trends of DELs. (**A**) Numbers of DELs in paired comparisons. (**B**) Change trends of DELs classified by main lipid subclasses during hepatocarcinogenesis. Red lines, upregulation; blue lines, downregulation; gray lines, nonsignificant change. Table S4 shows the detailed information of DELs. The symbol "/" means "versus." The abbreviations and descriptions are the same as those in the legend of Figure 1.

2.5. Common and unique DELs involved in sex-dependent hepatocarcinogenesis

Venn diagrams showed overlapping DELs between internal group comparisons in males and females, respectively (Figure 5A; Table S4). DELs that changed significantly in at least two pairs of comparisons were further classified into four categories to describe their variation trends in hepatocarcinogenesis: positively (a) or negatively (c) associated with HCC; positively (b) or negatively (d) associated with *Ras* oncogene (Figure 5B). Further, common and unique DELs between sexes were identified in the four categories (Figure 5B).

Figure 5. Common and unique DELs during sex-dependent hepatocarcinogenesis. (**A**) Venn analysis of DELs in both sexes. The symbol "/" means "versus." (**B**) Change pattern analysis of DELs during

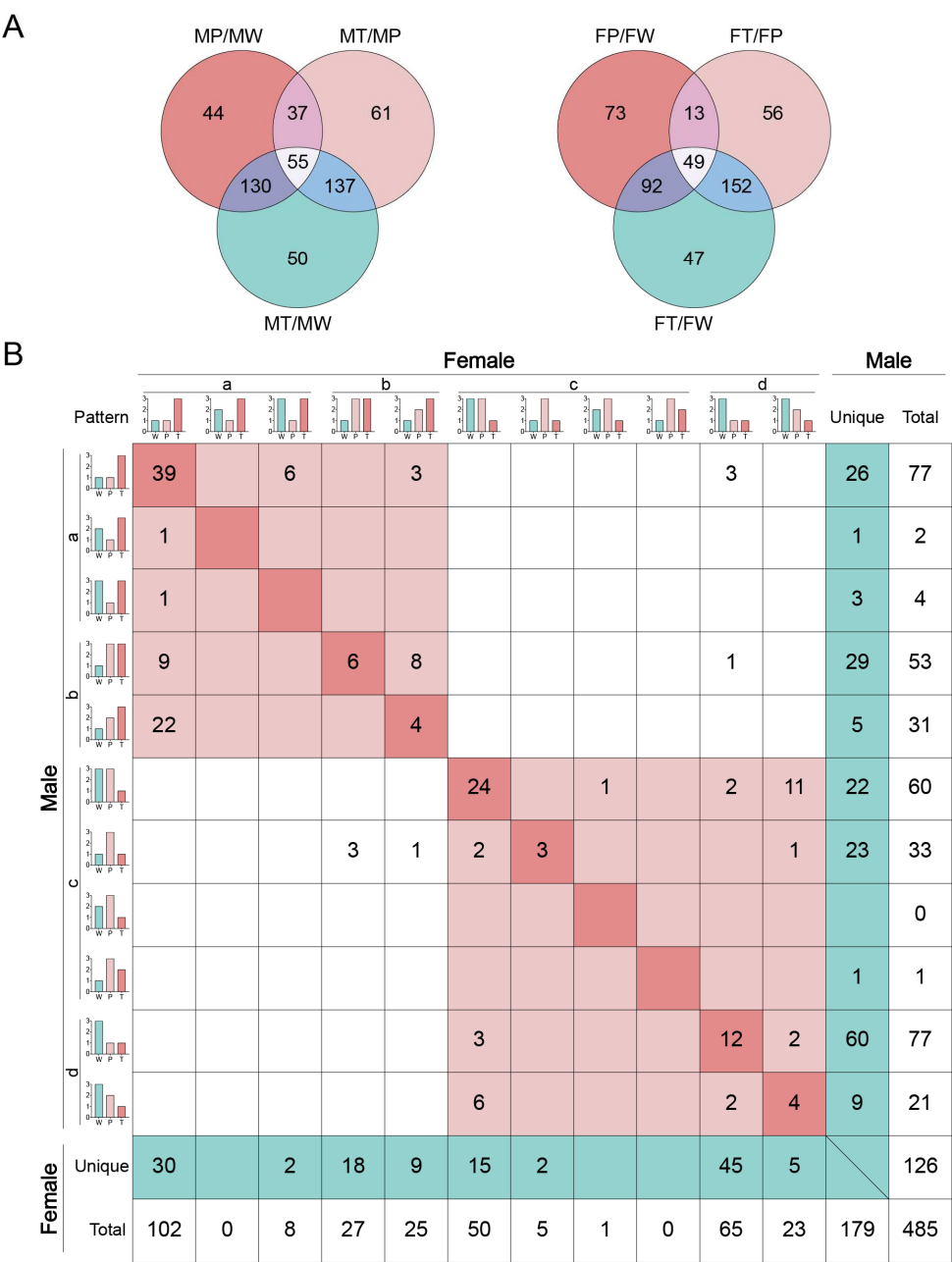hepatocarcinogenesis in both sexes. The related detailed information is shown in Table S3. DELs positively (a) or negatively (c) correlating with HCC represent lipids significantly elevated or reduced in T compared to P and/or W, respectively. DELs positively (b) or negatively (d) correlating with the Hras12V oncogene represent lipids significantly elevated or reduced in P and T compared to W, respectively. In the schematic diagram of the expression pattern, the numbers 1, 2, and 3 represent the graded and significant expression levels. The colored columns represent the significantly changed levels compared to at least one group in the same pattern. The deep red boxes indicate completely overlapping DELs between sexes in the same change pattern. The light red boxes indicate DELs with similar change patterns. The green boxes indicate unique DELs between sexes. The abbreviations and descriptions are the same as those in the legend of Figure 1.

This classification method has been described in detail in our previous study [16]. Briefly, in category (a), DELs play a positive role in HCC. Most of them belong to "⌁" model (refer to Table 1 for a description of this and the following symbols), indicating their weak responses to the *Ras* oncogene. The remaining DELs belong to "⋁" model, indicating they responded negatively to the *Ras* oncogene and, therefore, may be suppressed by the cancer prevention system in precancerous hepatocytes. In category (c), DELs play a negatively role in HCC. Among them, the DELs belonging to "⌄" model had a weak response to *Ras* oncogene, and the DELs belonging to "⋀" model responded positively to the *Ras* oncogenes expression in hepatocytes and, thus, may be activated by the cancer prevention system in precancerous hepatocytes. Categories (b) and (d) indicate that DELs respond positively or negatively to *Ras* oncogene expression in hepatocytes and hepatoma cells, respectively.

We screened a total of 485 DELs, including 359 in male mice and 306 in female mice. 180 DELs were common to both sexes. 179 and 126 DELs were exclusive to male mice and female mice, respectively. Males had significantly more unique DELs than females, which is consistent with our previous proteomics findings [16], suggesting that dysregulation of lipid metabolism is more strongly inhibited in female mice. Among the common DELs in both sexes, 99 were within the red regions of (a) and (b) (49 with completely same variant trends [diagonal line]) and correlated positively with HCC, while 73 were within the red regions of (c) and (d) (43 with completely same variant trends [diagonal line]) and correlated negatively with HCC (Figure 5B).

2.6. Roles of glycerolipid and glycerophospholipid metabolisms in HCC in both sexes

Among the 99 common DELs in categories (a) and (b), 77 (36 TGs, 12 TG-Os, 29 DGs) were glycerolipids. Among the 73 common DELs in classes (c) and (d), 49 (23 PCs, 10 LPCs, 4 PEs, 1 LPE, and others) were glycerophospholipids (Figure 5B). Thus, glycerolipid and glycerophospholipid metabolisms correlated positively and negatively with HCC in both sexes, respectively. Owing to the complex situations in W relative to P and/or T, which showed sexually dimorphism, and consistent change trends in T relative to P in both sexes (Figure 4B), the key enzymes related to glycerolipid and glycerophospholipid metabolic pathways were further verified in P and T of Ras-Tg by RT-qPCR (Figure 6), and data for W were not included. Generally, the significantly increased glycerolipids DG and TG in T may result from the transition among them with fueling FAs by endogenous biosynthesis and extracellular uptake by elevated key enzymes *Scd2*, *Acsl4*, *Acsl5*, and *Lpl*. Additionally, reduced *Cept1*, *Chpt1*, *Pcyt2*, *Selenoi*, and *Ptdss1* expressions may result in accumulation of DG and depletions of PC, PE, and PS in T simultaneously. Moreover, the significant rise in *Pla2g2e* expression may further led to the depletion of PC in T.
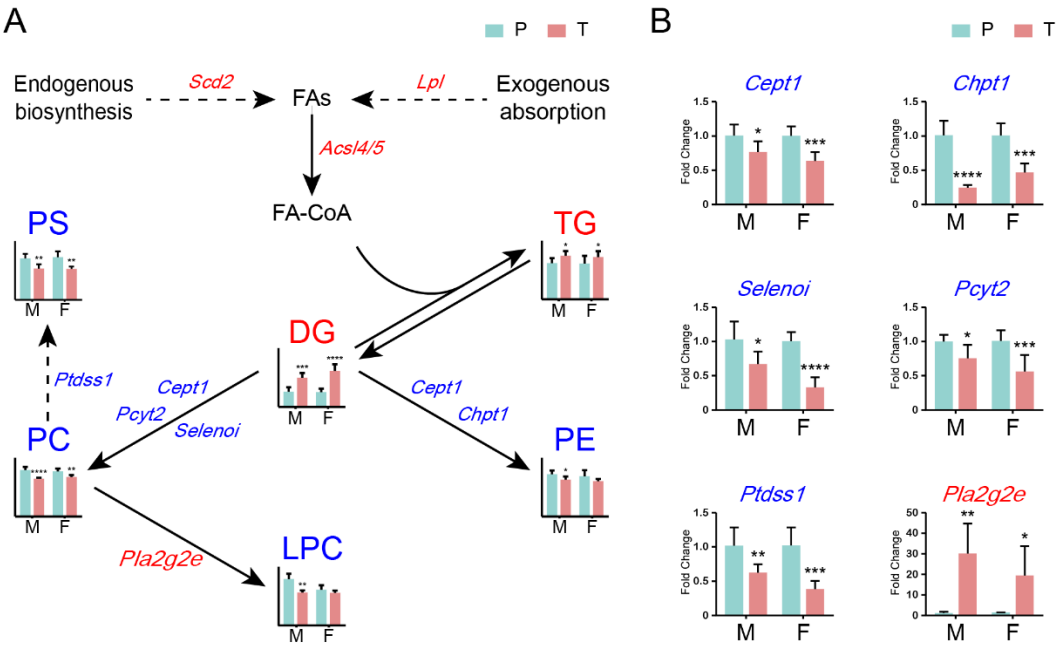
Figure 6. Roles of the glycerolipid and glycerophospholipid metabolic pathways in HCC in both sexes. (**A**) Schematic diagram of the glycerolipid and glycerophospholipid metabolic pathway changes in T relative to P of both sexes. Enzyme symbols are italicized. Red and blue lipids and enzymes indicate upregulation and downregulation in T relative to P, respectively. (**B**) RT-qPCR results of changes in the key enzymes involved in glycerolipid and glycerophospholipid metabolisms at the mRNA level. Changes in *Scd2*, *Lpl*, *Acsl4* and *Acsl5* at mRNA levels are shown in Figure 3. The abbreviations and descriptions are the same as those in the legend of Figure 1. The data are expressed as the mean ± SD. *, $p < 0.05$; **, $p < 0.01$; ***, $p < 0.001$; ****, $p < 0.0001$. n = 6.

2.7. Converging trend of lipid compositions during hepatocarcinogenesis between sexes

To investigate the sex disparity in lipid metabolisms in lateral comparisons, the difference in lipid compositions between sexes in W, P, and T were analyzed. First, the unsupervised hierarchical clustering showed that, although MW and FW were clustered far from each other, sexes showed close clustering in P and T, indicating a converging trend between sexes in lipid compositions of P and T (Figure 7A). Consistently, PCA showed that, although FW and MW were clearly separated, sexes showed gradual overlap in P and T (Figure 7B). Particularly, far fewer DELs were detected in comparisons of FP/MP and FT/MT than in that of FW/MW according to volcano plots and OPLS-DA analysis (Figures 7C and S5; Table S5). These data implied that the *Ras* oncogene expression and HCC development significantly narrowed the differences in hepatic lipid compositions between sexes.
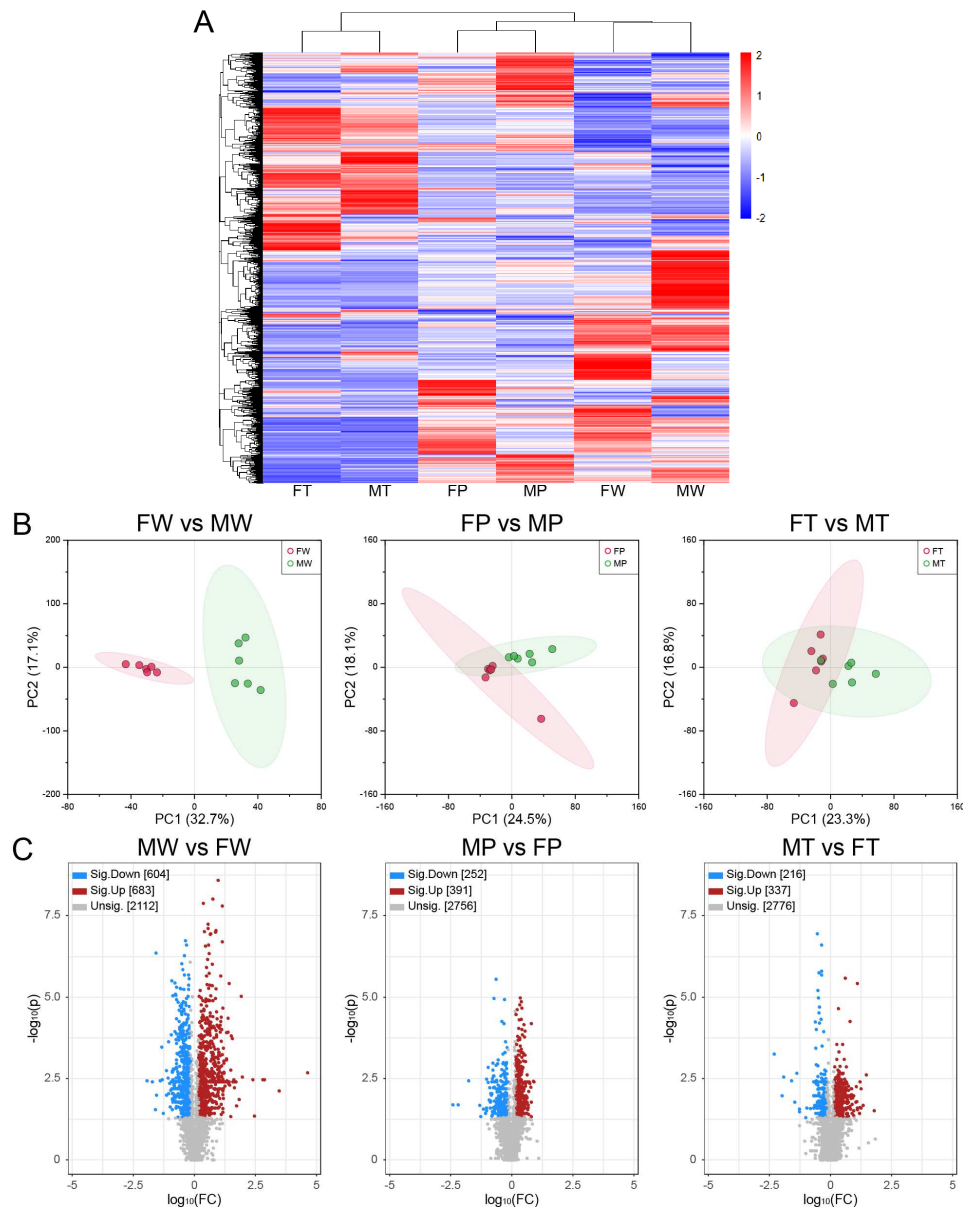
Figure 7. Lateral comparisons showing a converging trend during hepatocarcinogenesis between sexes. (**A**) Unsupervised hierarchical clustering based on lipidomics data. Red and blue indicate elevated and reduced lipid levels, respectively. The expression level of lipids in each group is the average of six individual samples in the same group. (**B**) PCA score plots based on lipidomics data. Green dots, male individuals; red dots, female individuals. (**C**) The volcano plots show DELs in lateral comparisons between sexes. Red dots, upregulation; blue dots, downregulation; gray dots, unchanged lipid levels; FC, foldchange. n = 6. Detailed data related to DELs are shown in Table S5. The abbreviations and descriptions are the same as those in the legend of Figure 1.

3. Discussion

Glycerolipids are involved in cell functions and cancer progression [17]. TG, an important compound for energy storage, is significantly elevated in both human and mouse HCC for rapid growth of hepatoma [18,19]. DG, a signaling molecule related to tumor promotion and carcinogenesis through activation of protein kinase C, is also elevated in HCC [19,20]. Consistently, our data showed that the levels of TG and DG were elevated in HCC (Figures 2A, 4B and S2). This was further supported by the fact that the upregulated key enzymes prompt adequate FA supplementation in HCC (Figure 6). Further, glycerolipids were concentrated in zone 3 of the hepatic lobules, which coincided with the original location of hepatic tumorigenesis (data not shown), indicating that the

12

accumulation and inhomogeneous distribution of glycerolipids may be closely related to hepatocarcinogenesis. Laboratory investigations of the underlying mechanisms are underway.

Glycerophospholipids perform biological functions, such as biofilm composition and signal transduction, and their metabolic dysregulation affects cancer progression [21]. They are elevated in many types of cancer [21]. However, in HCC, their metabolic alteration is complicated. Glycerophospholipid profiles in HCC and adjacent liver tissues differ across clinical reports. In some reports, the total glycerophospholipid concentration and/or the levels of their subclasses were significantly or nonsignificantly lower in HCC tissues than in adjacent tissues [22–24]. However, in other reports, PC and PE levels were elevated in HCC [25]. Because the etiological effects on clinical HCC are complex and difficult to distinguish, animal models are powerful tools to determine the different changes in glycerophospholipid profiles of HCC in response to different etiologies. In a mouse model, HCC induced by activated mammalian target of rapamycin (mTOR) signal transduction specifically resulted in reduced PC and PE levels and elevated PI and CL levels [26]. However, in HCC induced by diethylnitrosamine injections, the levels of PC, PE, PS, and PI did not differ significantly from those of surrounding tissues [19].

In the present study, the proportion and relative level of total glycerophospholipids were lower in T than in P in both sexes (Figures 2B and S2). PC, PE, LPC and PS levels were lower in T than in P (the decreasing trend of PE and LPC in females did not reach the level of significance), consistent with the overall trend (Figures 2B). These findings were further supported by the downregulated key enzymes in glycerophospholipid synthesis (Figure 6). Consistent with these findings, a choline deficiency diet may lead to HCC, and dietary PC supplementation can induce apoptosis to prevent HCC [27]. Additionally, reduced PC synthesis in human HCC cells increases the nuclear localization of SREBP-1 and lipogenesis [28]. Contrary to the decreasing trend in total glycerophospholipid levels, PI did not change significantly or even increased slightly in T compared with P (Figure 2B). Several phosphorylated PIs not included in the DELs in this study were obviously higher in T than in P (e.g., PIP2 O-39:3, p = 0.098 in males and p = 0.051 in females) (Table S3), and PIP2 is a direct substrate of phosphoinositide 3-kinase (PI3K). Consistent with these findings, PIs are often exploited by cancer cells to fuel pro-proliferative signaling, such as the PI3K/Akt/mTOR signaling pathway that is involved in tumorigenesis and progression of HCC [29,30]. Thus, disorders of glycerophospholipids may be involved in *Ras* oncogene-induced HCC and provide important clues for the clinical investigation of Ras signaling-involved HCC.

MUFAs promote cancer cell survival by inducing autophagy, enhancing cell membrane turnover, affecting intracellular signaling and gene transcription, and increasing energy production [31]. In human HCC, the MUFA levels are increased [32]. Accordingly, the expression of stearoyl-CoA desaturase-1 (SCD1), a key enzyme that converts SFA into MUFA, is up-regulated [33], and can even be used as a biomarker for the progression and prognosis of HCC [4]. Additionally, suppression of SCD1 inhibits the proliferation of human HCC cell lines by depleting MUFA [34]. Moreover, SCD1 consumes SFA and enables cancer cells to escape cell stress response and apoptosis [31,35]. Consistently, MUFA levels are elevated in mouse HCC [36]. In several studies, SCD2 undergoes significant upregulation regardless of SCD1 changes and is involved in pro-carcinogenic processes in mouse HCC induced by various factors, although SCD1 is the major isoform in the adult mouse liver [37–39]. This finding was further confirmed in the present study. The level of MUFA were elevated in HCC of Ras-Tg mice (Figure 3A,B). Accordingly, the expression of SCD2 was strongly upregulated (Figure 3C,D). Additionally, oleic acid (C18:1) drives HCC progression [40]. Among the MUFAs in the present study, oleic acid, as the main product of SCD, was significantly elevated (Figure 3C). These data combined with the published evidences suggested that SCD-induced upregulation of MUFA and oleic acid were involved in the occurrence and development of HCC. Therefore, targeted drug therapy involving MUFA may be an effective clinical treatment of HCC.

Additionally, the optimal MUFA/PUFA ratio is necessary to maintain normal biophysical properties of cell membranes and cell function, and its imbalance is responsible for many diseases, including HCC [32,41]. PC is the most abundant glycerophospholipid in cell membrane. In human and rodent HCC, PUFA-PC levels are reduced, while MUFA-PC levels are significantly elevated

compared to peri-tumor tissues [42]. A higher MUFA/PUFA ratio may result from oxidative stress in many tumors, while reduced binding of PUFA to membrane glycerophospholipids promotes resistance to lipid peroxidation and iron death in HCC [32]. This study also showed a significantly higher MUFA-PC/PUFA-PC ratio (Figure S2), supporting the involvement of the MUFA/PUFA ratio in membrane PC in HCC.

Sex disparities in hepatocarcinogenesis have been well recognized. However, whether or not sex disparity is present in developed HCC remains controversial. As sex hormones are involved in normal hepatocyte function as well as hepatocarcinogenesis, HCC may be suitable for resistance hormone therapy [43]. In one study, 17-β-estradiol and its compounds diethylstilbestrol, tamoxifen, and genistein-induced apoptosis in human hepatoma Hep3B cells [44]. In an animal model, cyproterone acetate inhibited the growth of androgen receptor-positive HCC transplanted in nude male mice [45]. In some studies, tamoxifen improved survival in patients with advanced HCC. However, in most studies, HCC was not a sex hormone-responsive tumor clinically because once the tumor developed, the anti-estrogen or anti-androgen therapy showed no anti-tumor effect or survival benefit [43,46]. Differences in protein expression profiles were significantly reduced in T compared to P or W between sexes [16]. Correspondingly, the expressions of androgen receptor (Ar) and estrogen receptor 1 (Esr1) and their corresponding genes changed significantly during hepatocarcinogenesis and finally resulted in no differences in T between sexes [16]. Consistently, the present study showed significantly attenuated differences in lipid profiles of T between sexes (Figure 7). These data suggested that sex characteristics in developed HCC were significantly attenuated, which supported the clinical loss of efficacy of sex hormone-dependent therapy.

Although the aforementioned evidence showed convergence in developed HCC, sexes showed significant differences during carcinogenesis. Because HCC is generally found late, collecting clinical samples of early liver lesions is difficult for systematic studies on the role of lipid metabolism disorders in the occurrence of sex-biased HCC. This was the first study to systematically describe the differential lipid metabolism disorder between sexes in hepatocarcinogenesis. Our data showed that in male mice, P had obviously higher glycerolipid and glycerophospholipid levels compared to W. However, in female mice, glycerolipid levels were significantly reduced, but glycerophospholipid levels did not change (Figure 2). In addition, male mice had a higher number of DELs than female mice in P/W comparisons, especially up-regulated DELs (Figure 4). This male-biased dysregulation of lipid metabolism has also been described in human HCC in that Liver X Receptor (LXR) and Retinoid X Receptor (RXR), which regulate lipid metabolism, are activated only in men with HCC [47]. These evidences suggest that lipid disorders in men are associated with male-biased HCC.

The male and female livers respond differently to the *Ras* oncogene. As aforementioned, more severe lipid disorganization in the male liver promotes the male propensity for HCC development. In addition, sex-dimorphic gene expression in the male and female livers [48], which translates into sex-specific differences in lipids, drugs, steroid hormones, and the xenobiotics metabolism [49], causes the sex bias in HCC. Our study showed different protein expression profiles between the wild-type male and female mouse livers [16], significant differences in lipid characteristics in W of the male and female mice, more abundant glycerolipids and fewer sphingolipids in the female livers (Figure 2, Table S2). Although the levels of some lipid species in W varied significantly between sexes, these differences were reduced in the context of Ras oncogene expression (Figures 7 and S2; Table S5). Except for PA, LBPA, and LPC, none of the lipid subclasses in P differed significantly between sexes (Table S2), indicating the homogeneity of hepatic lipid levels in male and female mice harboring the *Ras* oncogene. In our previous study, the *Ras* oncogene expression reduced the sex disparity in hepatocytes by attenuating sex hormone-related pathways and thereby attenuating the influence of sex hormones on hepatocarcinogenesis [16]. However, Ar and Esr1 still showed sexually dimorphic expressions in P [16], suggesting that Ras activation may affect lipid disorders in male mice through pathways other than the sex hormone pathway.

Lipids are the main component of organisms and cells and highly diverse in structure and distribution. Moreover, lipid metabolism is a complex network involving multiple isozymes and multifunctional enzymes. Understanding the biological relevance of this diversity and why cancer is

associated with severe lipid disorders are fundamental challenges in biology. Further studies integrating multiomics analyses, such as genomics, transcriptomics, proteomics, metabolomics, and functionomics, are required and would provide multiple perspectives to improve our understanding of disordered lipid metabolisms in hepatocarcinogenesis with sex disparity. In addition, owing to the male predilection of HCC in the Ras-Tg model, 9-month-old male and 15-month-old female mice were selected to achieve our research goals. However, age may be a factor affecting the results of the analysis. Moreover, lipid metabolism, especially in liver tissue, is strongly influenced by fluctuations in plasma sex hormones during the oestrus cycle for the female cohort. Therefore, oestrus cycle should be considered in future studies.

4. Conclusions

This was the first systematic study on sexually dimorphic lipid alterations in response to *Ras* oncogene-induced hepatocarcinogenesis. These data provide important information for lipid metabolic reprogramming in male-biased hepatocarcinogenesis and clues for clinical therapy and the underlying mechanisms.

5. Materials and Methods

5.1. Animals, sampling, and histopathological examination

Gender-dependent HCC model mice induced by hepatocyte-specific expression of Hras12V oncogene (Ras-Tg, C57BL/6J background) and wild-type non-Tg mice (Wt, C57BL/6J background) were housed at the Experimental Animal Center of Dalian Medical University. After euthanasia of the mice, the livers were washed with cold PBS. A portion of tissues were fixed in 4% paraformaldehyde fixative and examined histopathologically using the method described by Frith and Ward [50]. The remaining tissues were cut into small pieces and immediately frozen in liquid nitrogen. The details of methods have been described in detail in our previous studies [14,16]. All animal handling procedures were performed according to protocols approved by the Animal Care and Use Committee of Dalian Medical University (approval code, L2016189; approval date: Des. 18, 2016). The pathological diagnosis confirmed tissues were selected for the subsequent experimental procedures.

5.2. Experimental design and DELs screening

Since male (M) Ras-Tg develop HCC at a relatively early stage (8–9 months of age) with a high incidence (almost 100%) compared to females (F) (over 15 months of age and 30% incidence) [12,14], 9-month-old (9M) Ras-Tg and Wt males, 15-month-old (15M) Ras-Tg and Wt females were selected. The peri-tumor tissues (P) and hepatocellular carcinoma (T) of Ras-Tg and normal liver tissues of Wt (W) in both sexes (n = 6 for each group, total of 36 tissue samples) were used for lipidomic study. Then, lipid extracts from samples were subjected to UPLC-MS/MS to identify and quantify the lipid compositions (Figure 1A). Further, the differentially expressed lipids (DELs) were obtained by univariate and multivariate statistical analyses based on the criterion of $p < 0.05$, fold change > 1.5, VIP > 1.

5.3. Nontargeted lipidomics analysis based on UPLC-MS/MS

Approximately 90 mg of tissue samples were placed into 2 mL QSP tubes, and their weights were accurately recorded. All samples were washed with cold PBS before proceeding, and all liquid was aspirated after washing. Then 400 μL of 75% methanol-water solution (including internal standard) was added to the tube, vortexed for 1 min, and the beads were added and ground at 50 Hz for 4 min. 1 mL of MTBE was added, vortexed for 1 min, and shaken for 1 h. 250 μL of water was added, vortexed for 1 min, left to stand for 10 min, and centrifuged at 14000 g for 15 min at 4ed to the tube, vortexed for 1 min, and the beads were added and ground at 50 Hz for 4 min. 1 mL of MTBE was added, vortexed for 1 min, ad with 120 μL of acetonitrile: isopropanol: water solution (65: 30: 5), and the supernatant after centrifugation was used for positive and negative ion mode analysis. Blank

control samples were acetonitrile: isopropanol: water solution (65: 30: 5). All samples were lyophilized and stored in liquid nitrogen vapor prior to analysis. All experimental manipulations were performed at low temperature or on ice.

QC samples were constructed from a portion of each of all tissue lipid metabolite extracts. All real samples were analyzed in random order and 1 QC sample was inserted to every 6 real samples analyzed to monitor the robustness of the experiment. The BEH C8 column (1.7 μm, 2.1×100 mm) was from Waters, USA. The temperature of the column was 55e temper random order and 1 Q μure of the column was 55e temper random order and 1 QC sample was inserted to every 6 real samples anal (containing 10 mM ammonium acetate), and the mobile phase B consisted of isopropanol: acetonitrile = 9:1 (v/v, containing 10 mM ammonium acetate), and the gradient elution was performed according to the procedure: 0-1.5 min, 32% (B); 1.5-15.5 min, 32%-85% (B); 15.6-18 min, 97% (B); 18.1-21 min, 32% (B).

Coupled mass spectrometry analysis was performed by Thermo Scientific Q Exactive using a HESI ion source with a primary full scan and a DDA secondary sub-ion scan mode. The Spray voltage and mass range for the positive ion mode were +3.5 kV and 300-2000 m/z, respectively, while the negative ion mode was -3.0 kV and 150-1500 m/z. The rest of the positive and negative ion mode mass spectrometry experimental conditions were the same, with a Capillary temperature of 300℃, an Aux gas heater temperature of 350℃, Sheath gas flow rate of 45 Arb, Aux gas flow rate of 10 Arb, S-lens RF level of 50, Full ms resolution of 70,000, MS/MS resolution of 17500, TopN of 8, and NCE/stepped NCE of 25%, 35%, 45%.

Peak picking and alignment were performed by MS-DIALsoftware, raw peak areas were further normalized by the internal standard method. Based on the retention time, m/z and MS2 fragments, MS-DIAL, LipidSearch and the internal database of Dalian Institute of Chemical Physics [51] were used for the annotation of lipid metabolites. The nomenclature of lipids was referred to the naming rules of LipidSearch and LIPID MAPS (https://www.lipidmaps.org/).

5.4. Data Processing

The metabolite features from the data when the proportion of non-missing elements are accounted for less than 80% among each biological group were excluded in order to decrease the risk of reducing variable size and losing potential differential metabolites. Low reproducibility variables in QC samples with RSD greater than 30% were removed. Variables with more than 50% missing values were removed and missing values were replaced with the smallest value in the variable. To eliminate the effect of sample volume variation on metabolic mass spectrometry characteristics, the data were normalized based on total peak area and sample weight.

5.5. Real time quantitative PCR

Total RNA was isolated by Trizol (Tiangen Biotechnology, Beijing, China) following the manufacturer's procedures. Reverse transcriptase PCR was performed using a reverse transcription system (Tiangen Biotechnology, Beijing, China) according to the manufacturer's protocol. Real Master Mix SYBR Green (Tiangen Biotechnology, Beijing, China) was used in a StepOne PlusTM Real-Time PCR system (Applied Biosystems) to quantitate mRNA expression. The primers for detecting the expression level of target genes are shown in Table S6. The expression levels of genes were calculated against the *Rpl35a*. Expression changes were calculated using the delta-delta CT method.

5.6. Statistics

Normality tests and significance tests for lipidomic data and experimental data were done by GraphPad Prism (version 8.0.1). The normality of the data was tested using the Shapiro-Wilk method. Normally distributed data were tested with Student's t-test, otherwise Mann-Whitney U-test was used. Each experiment was performed at least in 6 individuals in each group. Error bars indicated standard deviation (SD). $p < 0.05$ were considered significant.

Supplementary Materials: The following supporting information can be downloaded at the website of this paper posted on Preprints.org. Figure S1: Quality control of positive and negative ion mode experiments in this

study; Figure S2: Percentage changes in major lipid species during hepatocarcinogenesis; Figure S3: Fatty acid analysis of the major lipid species identified, DG, TG, TG-O, PC, LPC and PE; Figure S4: Volcano plots of longitudinally paired comparisons; Figure S5: Orthogonal projections to latent structures discriminant analysis (OPLS-DA) for longitudinal comparisons; Figure S6: OPLS-DA analysis for lateral comparisons between sexes; Table S1: Detailed information for identified lipids; Table S2: P-values for pairwise comparisons of lipid levels between males and females; Table S3: Detailed information of DELs by longitudinally paired comparisons among W, P, and T in males and females, respectively; Table S4: Detailed information of DELs in Venn analysis; Table S5: Detailed information of DELs by lateral paired comparisons in W, P, and T between sexes; Table S6: Primer sequences for RT-qPCR.

Author Contributions: Study conceptualization, J.C. and A.W.; methodology, J.H., H.L., N.M., H.D., Y.Z. and J.C.; formal analysis/investigation, J.H., H.L., J.C. and A.W.; writing—original draft preparation, J.H., H.L., J.C. and A.W.; writing—review and editing, C.J. and AG.W. All authors have read and agreed to the published version of the manuscript.

Data Availability Statement: The original contributions presented in the study are all included in the article/ Supplementary Material.

Conflicts of Interest: The authors declare that there is no conflict of interest.

Abbreviations

HCC, Hepatocellular carcinoma; Ras-Tg, Hras12V transgenic mice; Wt, wild-type mice; W, liver tissues of Wt; P, Peri-tumor tissues of Ras-Tg; T, HCC tissues of Ras-Tg; 9M, 9-month-old; 15M, 15-month-old; F, female; M, male; DELs, Differentially expressed lipids; PCA, Principal component analysis; VIP, Variable importance of projection; TG, triacylglycerol; TG-O, alkyldiacylglycerol; DG, diacylglycerol; PC, phosphatidylcholine; PE, phosphatidylethanolamine; PG, phosphatidylglycerol; PI, phosphatidylinositol; PS, phosphatidylserine; PA, phosphatidic acid; LBPA, lysobisphosphatidic acid; LPC, lysophosphatidylcholine; LPE, Lysophosphatidylethanolamine; LPI, Lysophosphatidylinositol; LPG, lysophosphatidylglycerol; SM, sphingomyelin; phSM, phytosphingosine; Cer, ceramide; FA, Fatty acid; SFA, Saturated fatty acid; UFA, Unsaturated fatty acids; MUFA, Monounsaturated fatty acid; PUFA, Polyunsaturated fatty acid.

References

1. El-Serag, H.B.; Rudolph, K.L. Hepatocellular carcinoma: epidemiology and molecular carcinogenesis. *Gastroenterology* **2007**, *132*, 2557-2576, doi:10.1053/j.gastro.2007.04.061.
2. Kodama, K.; Kawaguchi, T.; Hyogo, H.; Nakajima, T.; Ono, M.; Seike, M.; Takahashi, H.; Nozaki, Y.; Kawanaka, M.; Tanaka, S.; et al. Clinical features of hepatocellular carcinoma in nonalcoholic fatty liver disease patients without advanced fibrosis. *J Gastroenterol Hepatol* **2019**, *34*, 1626-1632, doi:10.1111/jgh.14608.
3. Sangineto, M.; Villani, R.; Cavallone, F.; Romano, A.; Loizzi, D.; Serviddio, G. Lipid Metabolism in Development and Progression of Hepatocellular Carcinoma. *Cancers (Basel)* **2020**, *12*, doi:10.3390/cancers12061419.
4. Budhu, A.; Roessler, S.; Zhao, X.; Yu, Z.; Forgues, M.; Ji, J.; Karoly, E.; Qin, L.X.; Ye, Q.H.; Jia, H.L.; et al. Integrated metabolite and gene expression profiles identify lipid biomarkers associated with progression of hepatocellular carcinoma and patient outcomes. *Gastroenterology* **2013**, *144*, 1066-1075 e1061, doi:10.1053/j.gastro.2013.01.054.
5. Zhang, F.; Du, G. Dysregulated lipid metabolism in cancer. *World J Biol Chem* **2012**, *3*, 167-174, doi:10.4331/wjbc.v3.i8.167.
6. Bian, X.; Liu, R.; Meng, Y.; Xing, D.; Xu, D.; Lu, Z. Lipid metabolism and cancer. *J Exp Med* **2021**, *218*, doi:10.1084/jem.20201606.
7. Wenk, M.R. Lipidomics: new tools and applications. *Cell* **2010**, *143*, 888-895, doi:10.1016/j.cell.2010.11.033.
8. Gedaly, R.; Angulo, P.; Hundley, J.; Daily, M.F.; Chen, C.; Evers, B.M. PKI-587 and sorafenib targeting PI3K/AKT/mTOR and Ras/Raf/MAPK pathways synergistically inhibit HCC cell proliferation. *J Surg Res* **2012**, *176*, 542-548, doi:10.1016/j.jss.2011.10.045.
9. Calvisi, D.F.; Ladu, S.; Gorden, A.; Farina, M.; Conner, E.A.; Lee, J.S.; Factor, V.M.; Thorgeirsson, S.S. Ubiquitous activation of Ras and Jak/Stat pathways in human HCC. *Gastroenterology* **2006**, *130*, 1117-1128, doi:10.1053/j.gastro.2006.01.006.

10. Chen, L.; Shi, Y.; Jiang, C.Y.; Wei, L.X.; Wang, Y.L.; Dai, G.H. Expression and prognostic role of pan-Ras, Raf-1, pMEK1 and pERK1/2 in patients with hepatocellular carcinoma. *Eur J Surg Oncol* **2011**, *37*, 513-520, doi:10.1016/j.ejso.2011.01.023.

11. Bartolacci, C.; Andreani, C.; El-Gammal, Y.; Scaglioni, P.P. Lipid Metabolism Regulates Oxidative Stress and Ferroptosis in RAS-Driven Cancers: A Perspective on Cancer Progression and Therapy. *Front Mol Biosci* **2021**, *8*, 706650, doi:10.3389/fmolb.2021.706650.

12. Wang, A.G.; Moon, H.B.; Lee, M.R.; Hwang, C.Y.; Kwon, K.S.; Yu, S.L.; Kim, Y.S.; Kim, M.; Kim, J.M.; Kim, S.K.; et al. Gender-dependent hepatic alterations in H-ras12V transgenic mice. *J Hepatol* **2005**, *43*, 836-844, doi:10.1016/j.jhep.2005.04.012.

13. Wang, A.G.; Moon, H.B.; Chae, J.I.; Kim, J.M.; Kim, Y.E.; Yu, D.Y.; Lee, D.S. Steatosis induced by the accumulation of apolipoprotein A-I and elevated ROS levels in H-ras12V transgenic mice contributes to hepatic lesions. *Biochem Biophys Res Commun* **2011**, *409*, 532-538, doi:10.1016/j.bbrc.2011.05.039.

14. Rong, Z.; Fan, T.; Li, H.; Li, J.; Wang, K.; Wang, X.; Dong, J.; Chen, J.; Wang, F.; Wang, J.; et al. Differential Proteomic Analysis of Gender-dependent Hepatic Tumorigenesis in Hras12V Transgenic Mice. *Mol Cell Proteomics* **2017**, *16*, 1475-1490, doi:10.1074/mcp.M116.065474.

15. Smith, P.F.; Zheng, Y. Applications of Multivariate Statistical and Data Mining Analyses to the Search for Biomarkers of Sensorineural Hearing Loss, Tinnitus, and Vestibular Dysfunction. *Front Neurol* **2021**, *12*, 627294, doi:10.3389/fneur.2021.627294.

16. Li, H.; Rong, Z.; Wang, H.; Zhang, N.; Pu, C.; Zhao, Y.; Zheng, X.; Lei, C.; Liu, Y.; Luo, X.; et al. Proteomic analysis revealed common, unique and systemic signatures in gender-dependent hepatocarcinogenesis. *Biol Sex Differ* **2020**, *11*, 46, doi:10.1186/s13293-020-00316-5.

17. Prentki, M.; Madiraju, S.R. Glycerolipid metabolism and signaling in health and disease. *Endocr Rev* **2008**, *29*, 647-676, doi:10.1210/er.2008-0007.

18. Lu, Y.; Chen, J.; Huang, C.; Li, N.; Zou, L.; Chia, S.E.; Chen, S.; Yu, K.; Ling, Q.; Cheng, Q.; et al. Comparison of hepatic and serum lipid signatures in hepatocellular carcinoma patients leads to the discovery of diagnostic and prognostic biomarkers. *Oncotarget* **2018**, *9*, 5032-5043, doi:10.18632/oncotarget.23494.

19. Haberl, E.M.; Pohl, R.; Rein-Fischboeck, L.; Horing, M.; Krautbauer, S.; Liebisch, G.; Buechler, C. Accumulation of cholesterol, triglycerides and ceramides in hepatocellular carcinomas of diethylnitrosamine injected mice. *Lipids Health Dis* **2021**, *20*, 135, doi:10.1186/s12944-021-01567-w.

20. Becker, K.P.; Hannun, Y.A. Protein kinase C and phospholipase D: intimate interactions in intracellular signaling. *Cell Mol Life Sci* **2005**, *62*, 1448-1461, doi:10.1007/s00018-005-4531-7.

21. Szlasa, W.; Zendran, I.; Zalesinska, A.; Tarek, M.; Kulbacka, J. Lipid composition of the cancer cell membrane. *J Bioenerg Biomembr* **2020**, *52*, 321-342, doi:10.1007/s10863-020-09846-4.

22. Liu, Z.; Zhang, Z.; Mei, H.; Mao, J.; Zhou, X. Distribution and clinical relevance of phospholipids in hepatocellular carcinoma. *Hepatol Int* **2020**, *14*, 544-555, doi:10.1007/s12072-020-10056-8.

23. Zhong, H.; Xiao, M.; Zarkovic, K.; Zhu, M.; Sa, R.; Lu, J.; Tao, Y.; Chen, Q.; Xia, L.; Cheng, S.; et al. Mitochondrial control of apoptosis through modulation of cardiolipin oxidation in hepatocellular carcinoma: A novel link between oxidative stress and cancer. *Free Radic Biol Med* **2017**, *102*, 67-76, doi:10.1016/j.freeradbiomed.2016.10.494.

24. Ismail, I.T.; Elfert, A.; Helal, M.; Salama, I.; El-Said, H.; Fiehn, O. Remodeling Lipids in the Transition from Chronic Liver Disease to Hepatocellular Carcinoma. *Cancers (Basel)* **2020**, *13*, doi:10.3390/cancers13010088.

25. Huang, Q.; Tan, Y.; Yin, P.; Ye, G.; Gao, P.; Lu, X.; Wang, H.; Xu, G. Metabolic characterization of hepatocellular carcinoma using nontargeted tissue metabolomics. *Cancer Res* **2013**, *73*, 4992-5002, doi:10.1158/0008-5472.CAN-13-0308.

26. Guri, Y.; Colombi, M.; Dazert, E.; Hindupur, S.K.; Roszik, J.; Moes, S.; Jenoe, P.; Heim, M.H.; Riezman, I.; Riezman, H.; et al. mTORC2 Promotes Tumorigenesis via Lipid Synthesis. *Cancer Cell* **2017**, *32*, 807-823 e812, doi:10.1016/j.ccell.2017.11.011.

27. Buechler, C.; Aslanidis, C. Role of lipids in pathophysiology, diagnosis and therapy of hepatocellular carcinoma. *Biochim Biophys Acta Mol Cell Biol Lipids* **2020**, *1865*, 158658, doi:10.1016/j.bbalip.2020.158658.

28. Walker, A.K.; Jacobs, R.L.; Watts, J.L.; Rottiers, V.; Jiang, K.; Finnegan, D.M.; Shioda, T.; Hansen, M.; Yang, F.; Niebergall, L.J.; et al. A conserved SREBP-1/phosphatidylcholine feedback circuit regulates lipogenesis in metazoans. *Cell* **2011**, *147*, 840-852, doi:10.1016/j.cell.2011.09.045.

29. Sun, E.J.; Wankell, M.; Palamuthusingam, P.; McFarlane, C.; Hebbard, L. Targeting the PI3K/Akt/mTOR Pathway in Hepatocellular Carcinoma. *Biomedicines* **2021**, *9*, doi:10.3390/biomedicines9111639.

30. Koundouros, N.; Poulogiannis, G. Reprogramming of fatty acid metabolism in cancer. *Br J Cancer* **2020**, *122*, 4-22, doi:10.1038/s41416-019-0650-z.

31. Pope, E.D., 3rd; Kimbrough, E.O.; Vemireddy, L.P.; Surapaneni, P.K.; Copland, J.A., 3rd; Mody, K. Aberrant lipid metabolism as a therapeutic target in liver cancer. *Expert Opin Ther Targets* **2019**, *23*, 473-483, doi:10.1080/14728222.2019.1615883.

32. Tan, S.L.W.; Israeli, E.; Ericksen, R.E.; Chow, P.K.H.; Han, W. The altered lipidome of hepatocellular carcinoma. *Semin Cancer Biol* **2022**, doi:10.1016/j.semcancer.2022.02.004.

33.   Calvisi, D.F.; Wang, C.; Ho, C.; Ladu, S.; Lee, S.A.; Mattu, S.; Destefanis, G.; Delogu, S.; Zimmermann, A.; Ericsson, J.; et al. Increased lipogenesis, induced by AKT-mTORC1-RPS6 signaling, promotes development of human hepatocellular carcinoma. *Gastroenterology* **2011**, *140*, 1071-1083, doi:10.1053/j.gastro.2010.12.006.

34.   Yao, Y.; Sun, S.; Wang, J.; Fei, F.; Dong, Z.; Ke, A.W.; He, R.; Wang, L.; Zhang, L.; Ji, M.B.; et al. Canonical Wnt Signaling Remodels Lipid Metabolism in Zebrafish Hepatocytes following Ras Oncogenic Insult. *Cancer Res* **2018**, *78*, 5548-5560, doi:10.1158/0008-5472.CAN-17-3964.

35.   Igal, R.A. Roles of StearoylCoA Desaturase-1 in the Regulation of Cancer Cell Growth, Survival and Tumorigenesis. *Cancers (Basel)***2011**, *3*, 2462-2477, doi:10.3390/cancers3022462.

36.   Griffitts, J.; Tesiram, Y.; Reid, G.E.; Saunders, D.; Floyd, R.A.; Towner, R.A. In vivo MRS assessment of altered fatty acyl unsaturation in liver tumor formation of a TGF alpha/c-myc transgenic mouse model. *J Lipid Res* **2009**, *50*, 611-622, doi:10.1194/jlr.M800265-JLR200.

37.   Miyazaki, M.; Dobrzyn, A.; Elias, P.M.; Ntambi, J.M. Stearoyl-CoA desaturase-2 gene expression is required for lipid synthesis during early skin and liver development. *Proc Natl Acad Sci U S A* **2005**, *102*, 12501-12506, doi:10.1073/pnas.0503132102.

38.   Li, L.; Wang, C.; Calvisi, D.F.; Evert, M.; Pilo, M.G.; Jiang, L.; Yuneva, M.; Chen, X. SCD1 Expression is dispensable for hepatocarcinogenesis induced by AKT and Ras oncogenes in mice. *PLoS One* **2013**, *8*, e75104, doi:10.1371/journal.pone.0075104.

39.   Chen, X.; Yamamoto, M.; Fujii, K.; Nagahama, Y.; Ooshio, T.; Xin, B.; Okada, Y.; Furukawa, H.; Nishikawa, Y. Differential reactivation of fetal/neonatal genes in mouse liver tumors induced in cirrhotic and non-cirrhotic conditions. *Cancer Sci* **2015**, *106*, 972-981, doi:10.1111/cas.12700.

40.   Seo, J.; Jeong, D.W.; Park, J.W.; Lee, K.W.; Fukuda, J.; Chun, Y.S. Fatty-acid-induced FABP5/HIF-1 reprograms lipid metabolism and enhances the proliferation of liver cancer cells. *Commun Biol* **2020**, *3*, 638, doi:10.1038/s42003-020-01367-5.

41.   Maulucci, G.; Cohen, O.; Daniel, B.; Sansone, A.; Petropoulou, P.I.; Filou, S.; Spyridonidis, A.; Pani, G.; De Spirito, M.; Chatgilialoglu, C.; et al. Fatty acid-related modulations of membrane fluidity in cells: detection and implications. *Free Radic Res* **2016**, *50*, S40-S50, doi:10.1080/10715762.2016.1231403.

42.   Hall, Z.; Chiarugi, D.; Charidemou, E.; Leslie, J.; Scott, E.; Pellegrinet, L.; Allison, M.; Mocciaro, G.; Anstee, Q.M.; Evan, G.I.; et al. Lipid Remodeling in Hepatocyte Proliferation and Hepatocellular Carcinoma. *Hepatology* **2021**, *73*, 1028-1044, doi:10.1002/hep.31391.

43.   De Maria, N.; Manno, M.; Villa, E. Sex hormones and liver cancer. *Mol Cell Endocrinol* **2002**, *193*, 59-63, doi:10.1016/s0303-7207 (02)00096-5.

44.   Huang, E.J.; Wu, C.C.; Huang, H.P.; Liu, J.Y.; Lin, C.S.; Chang, Y.Z.; Lin, J.A.; Lin, J.G.; Chen, L.M.; Lee, S.D.; et al. Apoptotic and anti-proliferative effects of 17beta-estradiol and 17beta-estradiol-like compounds in the Hep3B cell line. *Mol Cell Biochem* **2006**, *290*, 1-7, doi:10.1007/s11010-005-9000-y.

45.   Nagasue, N.; Yu, L.; Yamaguchi, M.; Kohno, H.; Tachibana, M.; Kubota, H. Inhibition of growth and induction of TGF-beta 1 in human hepatocellular carcinoma with androgen receptor by cyproterone acetate in male nude mice. *J Hepatol* **1996**, *25*, 554-562, doi:10.1016/s0168-8278 (96)80216-9.

46.   Barbare, J.C.; Bouche, O.; Bonnetain, F.; Raoul, J.L.; Rougier, P.; Abergel, A.; Boige, V.; Denis, B.; Blanchi, A.; Pariente, A.; et al. Randomized controlled trial of tamoxifen in advanced hepatocellular carcinoma. *J Clin Oncol* **2005**, *23*, 4338-4346, doi:10.1200/JCO.2005.05.470.

47.   Ma, J.; Malladi, S.; Beck, A.H. Systematic Analysis of Sex-Linked Molecular Alterations and Therapies in Cancer. *Sci Rep* **2016**, *6*, 19119, doi:10.1038/srep19119.

48.   Mayne, B.T.; Bianco-Miotto, T.; Buckberry, S.; Breen, J.; Clifton, V.; Shoubridge, C.; Roberts, C.T. Large Scale Gene Expression Meta-Analysis Reveals Tissue-Specific, Sex-Biased Gene Expression in Humans. *Front Genet* **2016**, *7*, 183, doi:10.3389/fgene.2016.00183.

49.   Bakiri, L.; Wagner, E.F. Mouse models for liver cancer. *Mol Oncol* **2013**, *7*, 206-223, doi:10.1016/j.molonc.2013.01.005.

50.   Frith, C.H.; Ward, J.M. A morphologic classification of proliferative and neoplastic hepatic lesions in mice. *J Environ Pathol Toxicol* **1979**, *3*, 329-351.

51.   Zhao, X., Zeng, Z., Chen, A., Lu, X., Zhao, C., Hu, C., Zhou, L., Liu, X., Wang, X., Hou, X., Ye, Y., Xu, G. Comprehensive Strategy to Construct In-House Database for Accurate and Batch Identification of Small Molecular Metabolites. *Anal Chem*. **2018**,*90 (12)*,7635-7643,doi: 10.1021/acs.analchem.8b01482.